

POWER SPECTRA AND MIXING PROPERTIES OF STRANGE ATTRACTORS

Doync Farmer, James Crutchfield, Harold Froehling,
Norman Packard, and Robert Shaw*

*Dynamical Systems Group
Physics Board of Studies
University of California, Santa Cruz
Santa Cruz, California 95064*

INTRODUCTION

Edward Lorenz used the phrase “deterministic nonperiodic flow” to describe the first example of what is now known as a “strange” or “chaotic” attractor.¹⁻³ Nonperiodicity, as reflected by a broadband component in a power spectrum of a time series, is the characteristic by which chaos is currently experimentally identified. In principle, this identification is straightforward: Systems that are periodic or quasi-periodic have power spectra composed of delta functions; any dynamical system whose spectrum is not composed of delta functions is chaotic.

We have found that, to the resolution of our numerical experiments, some strange attractors have power spectra that are superpositions of delta functions and broad backgrounds. As we shall show, strange attractors with this property, which we call *phase coherence*, are chaotic, yet, nonetheless, at least approach being periodic or quasi-periodic in a statistical sense. Under various names, this property has also been noted by Lorenz (“noisy periodicity”),⁴ Ito et al. (“nonmixing chaos”),⁵ and the authors.⁶ The existence of phase coherence can make it difficult to discriminate experimentally between chaotic and periodic behavior by means of a power spectrum. In this paper, we investigate the geometric basis of phase coherence and demonstrate that this phenomenon is closely related to the mixing properties of attractors.

The theory of dynamical systems provides two useful measures of chaos: the Kolmogorov entropy⁷ and the Lyapunov characteristic exponents.^{8,9} The application of this theory to strange attractors is not well understood, but it is at least a commonly expressed conjecture, supported by numerical evidence,¹⁰ that these quantities can be defined for strange attractors, and that the appropriately normalized Kolmogorov entropy is equal to the sum of the positive Lyapunov characteristic exponents.^{11,12} The presence of chaotic behavior in a dynamical system is signaled by a positive Kolmogorov entropy. We have discovered, however, that neither of these quantities distinguish between phase coherent and phase incoherent chaos. Since attractors with a long term average periodicity are intuitively “more orderly” than incoherent attractors, these quantities provide an inadequate measure of the chaotic properties of a strange attractor.

Phase coherent strange attractors may be the correct models for many physical systems. In Couette flow, for example, through certain parameter ranges, wavy Taylor

*D.F. would like to thank the Hertz Foundation for their support; J.C., N.P., and R.S. gratefully acknowledge the support of the National Science Foundation.

vortices preserve large scale order despite turbulent motion on smaller length scales within the vortices. A power spectrum of the fluid motion at a point reveals a sharp peak, which corresponds to azimuthal waves, superimposed on a broad background, which corresponds to small scale turbulence. (See Walden and Donnelly¹³ or Fenstermacher, Swinney, and Gollub¹⁴). Thus, this problem is of practical as well as theoretical interest.

DESCRIPTION OF PHASE COHERENCE

We will study three examples in detail. One of these is due to Lorenz,¹

$$\begin{aligned}\dot{x} &= 10y - 10x \\ \dot{y} &= -y - xz + Rx \\ \dot{z} &= xy - \frac{8}{3}z.\end{aligned}\tag{1}$$

When $R = 28$ we will refer to this as "the Lorenz attractor." The other two examples are due to Rössler,¹⁵

$$\begin{aligned}\dot{x} &= -(y + z) \\ \dot{y} &= x + ay \\ \dot{z} &= b + xz - cz.\end{aligned}\tag{2}$$

When $a = 0.343$, $b = 1.82$, and $c = 9.75$, we will refer to this as "the funnel," and, when $a = 0.2$, $b = 0.2$, and $c = 5.7$, as "the simple Rössler attractor." All of these are strange attractors with one positive Lyapunov exponent. Phase space projections and power spectra are shown in FIGURES 1, 2, and 3. Notice the contrast between a power spectrum of $x(t)$ of the Lorenz attractor, which is almost featureless (FIGURE 1b), and a power spectrum of the simple Rössler attractor (FIGURE 3b), which is composed of sharp peaks superimposed on a broad background. The peak at 0.17 and its harmonics are instrumentally sharp. The width is due solely to the finite length of the data; sine waves added to the data give peaks just as broad. Thus, to the resolution of our experiments, it is a good approximation to assume that these peaks are delta functions. The linearity of the Fourier transform then implies that $x(t)$ of the simple Rössler system can be written as the sum of a periodic and a nonperiodic part:

$$x(t) = x_p(t) + x_{np}(t).\tag{3}$$

This implies that the autocorrelation function may be written as the sum of a component that decays to zero and a periodic component that does not decay.

For signals of the form of equation 3, the nonperiodic component introduces some uncertainty into the measurement of the time for one cycle of the periodic component. On the other hand, this uncertainty is the same as the uncertainty in a measurement of the time for many cycles. The uncertainty in phase does not grow with time. This is the origin of the term "phase coherence."

In order to quantify this property, we introduce the following statistical quantity:

$$\Delta T(i) = \lim_{N \rightarrow \infty} \frac{1}{N} \sum_{n=1}^N |T_n(i) - T_{ave}(i)|.\tag{4}$$

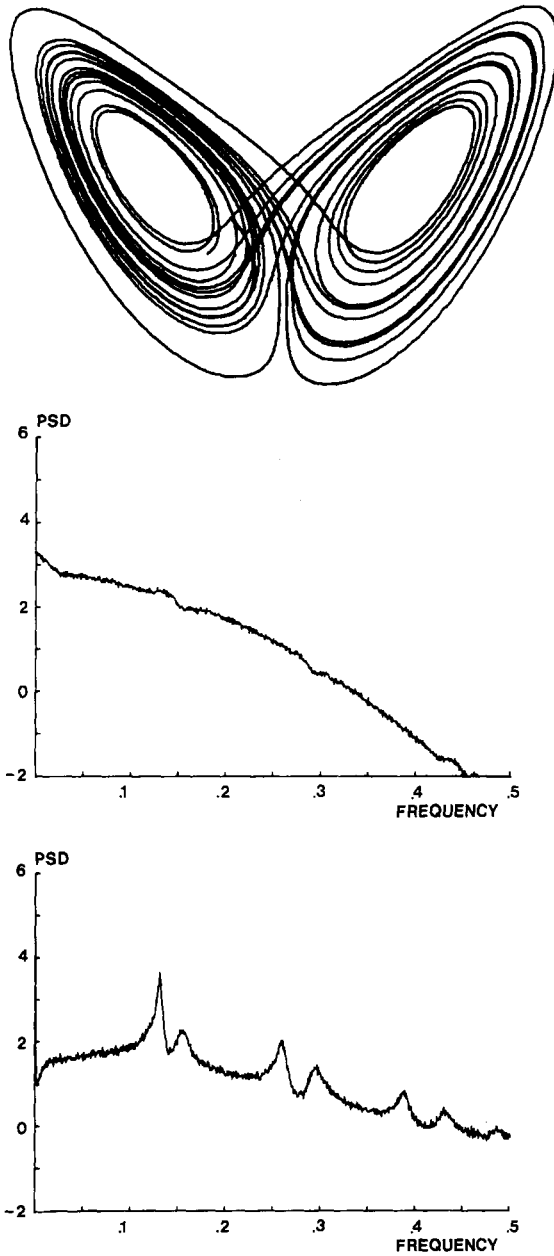


FIGURE 1. A Lorenz attractor with $R = 28$. (a) An xz projection of a sample trajectory. (b) A power spectrum of $x(t)$. (c) A power spectrum of $z(t)$.

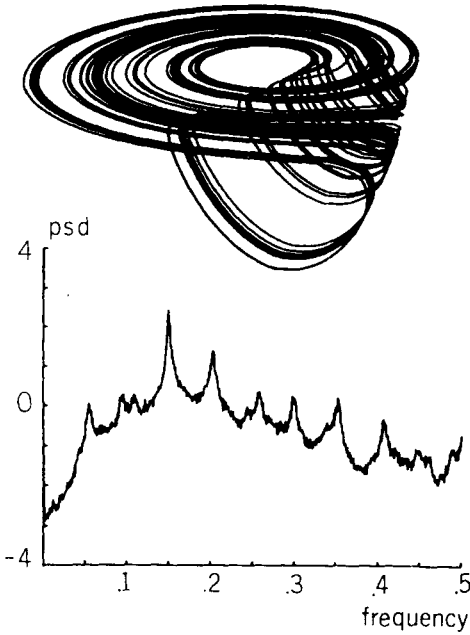


FIGURE 2. "The Funnel," equation 2 with $a = 0.343, b = 1.82, c = 9.75$. (a) A perspective view of a sample trajectory. (b) A power spectrum of $x(t)$.

$T_{ave}(i)$ is the average time for i maxima to recur, and $T_n(i)$ is the time for i maxima to recur during a particular (the n th) trial; i may be thought of as a discrete time. Insofar as maxima occur at a particular "phase," this statistic measures the mean cumulative deviation of the phase after a time i . For convenience in performing machine computations, we chose to use absolute values rather than a root-mean-square statistic. Note that, when measured in units of $T_{ave}(1)$, ΔT is independent of a change of timescale, $t \rightarrow t'$, in the equations under study.

The results of applying this statistic to $y(t)$ and $z(t)$ of the Lorenz attractor and to $x(t)$ of the simple Rössler attractor are shown in FIGURE 4. $y(t)$ and $z(t)$ of the Rössler give results similar to $x(t)$; $x(t)$ of the Lorenz attractor is similar to $y(t)$. Notice that ΔT of the Rössler attractor grows a negligible amount after 1000 cycles. On a greatly expanded scale, ΔT for $i = 1$ has a small but finite value of 0.015 average periods. However, at the resolution of our experiment, the increase after 1024 cycles in ΔT for the simple Rössler attractor is negligible. This demonstrates that the fractional spreading of phase for the simple Rössler attractor is less than 0.015/1024, or, equivalently, that the peaks in the power spectrum of this attractor are sharp to at least one part in 68,000.

An example of a bifurcation from a coherent to an incoherent attractor is presented in FIGURE 5 (see also Reference 5). Through a wide range of parameter values, the phase coherence is instrumentally sharp and the attractor keeps the topological form of the simple Rössler attractor seen in FIGURE 5a. At $a = 0.18$, the topology of the attractor changes sharply, and the spectrum broadens, as seen in FIGURE 5c. This continues in a smooth manner until the spectrum takes the broadband form seen in FIGURE 5f.

It appears that instrumentally sharp phase coherence is not atypical of simple dynamical systems. E. N. Lorenz has observed this phenomenon in equations 1 at $R = 200$.⁴ On the other hand, it is unclear exactly what geometrical features distinguish instrumentally sharp phase coherence. For example, we have found another attractor with the same topology as the simple Rössler attractor, which is only partially phase coherent. Furthermore, a sufficiently strong perturbation of (2) can broaden the peak of the simple Rössler attractor, even though the topology remains the same.

There is often a connection between the occurrence of phase coherence and the period-doubling bifurcation sequence.⁶ The strange attractors near the accumulation point of a period-doubling bifurcation sequence are bandlike, or semiperiodic,⁴ and are always somewhat phase coherent. For example, consider an attractor composed of very thin bands. The motion on the attractor takes place approximately on a closed curve, causing a peak in the power spectrum. However, the phase coherence of different dynamical systems varies considerably and depends on factors that we have not been able to determine. Phase coherence has also been observed with no easily

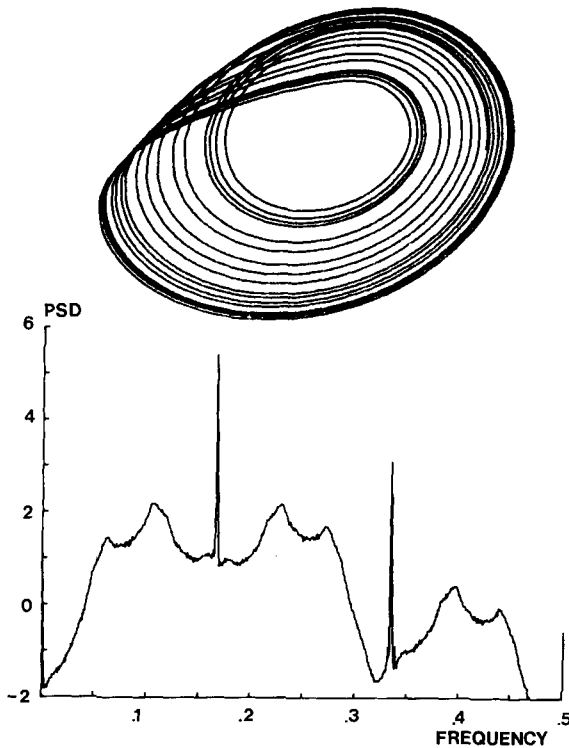


FIGURE 3. The simple Rössler attractor, equation 2. In all of the examples discussed in the text we used $a = 0.2$, $b = 0.2$, and $c = 5.7$, except for FIGURE 3b, in which we used $b = 0.4$. (a) An xy projection of a sample trajectory. (b) A power spectrum of $x(t)$. Note that, because of the symmetry of the broad component about the peak, a stronger statement than that of equation 3 can be made about the form of $x(t)$. See Appendix II.

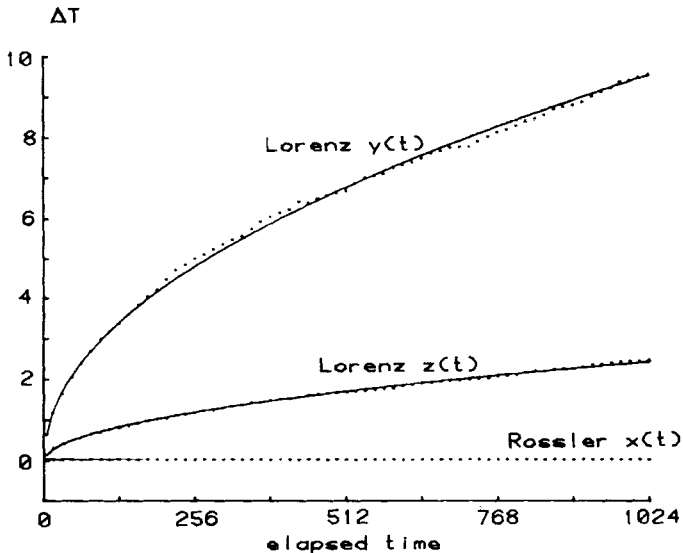


FIGURE 4. Loss of phase coherence ΔT for $x(t)$ of the Lorenz attractor, $z(t)$ of the Lorenz attractor, and $x(t)$ of the simple Rössler attractor. To make this plot independent of a rescaling of the time in the equations, both vertical and horizontal axes are shown in units of the average time between maxima. The number of samples, N , was 1543 and 911 for $y(t)$ and $z(t)$ of the Lorenz attractor, and 1330 for the Rössler attractor. Best fits for curves of the form $a \cdot t^b$ are shown for the Lorenz attractor. For $y(t)$, $a = 0.309$, $b = 0.516$; for $z(t)$, $a = 0.0679$, $b = 0.495$.

discernable nearby period-doubling bifurcation, for example, Walden and Donnelly's reemergent peak.¹³ Thus, it appears that association with a period-doubling sequence implies some degree of phase coherence, but is not a necessary condition for its occurrence.

MIXING

In order for phase coherence to be seen in a numerical simulation, or observed in a physical system, the property of phase coherence must persist in the presence of small fluctuations. A small fluctuation can be modeled by an ensemble, or "cloud," of neighboring points; the behavior of the system with fluctuations can then be studied by following the points in the ensemble. As we shall see, the long-time behavior of these trajectories in fact determines the coherence properties of the attractor. Thus, the coherence of a dynamical system is fixed by its response to small fluctuations, which is closely related to its mixing properties.

If an attractor is *mixing*, a cloud of initially adjacent points will be spread throughout the attractor by the flow. The density of points eventually approaches an *asymptotic probability distribution*, which is also called an *invariant measure* because

it is carried into itself by the flow. The final distribution is independent of the location or nature of the initial ensemble and, as it is approached, no information about the initial time or position of the ensemble remains. But, if an attractor has a high degree of phase coherence, it must propagate phase information far into the future. This in turn implies, at best, very slow mixing by the flow. The cloud of points of the ensemble must remain localized for a very long time; their distribution approaches an invariant measure slowly, if at all.

Each of the strange attractors studied here has a spectrum of Lyapunov characteristic exponents consisting of one positive exponent, one negative exponent, and one exponent equal to zero. The positive exponent implies that the size of a localized cloud of points will grow (on the average) exponentially in a direction transverse to the flow. The zero exponent implies that, on the average, in a direction along the flow, the cloud will neither grow nor shrink. The negative exponent implies that, in directions transverse to the attractor, the cloud can only shrink. With the

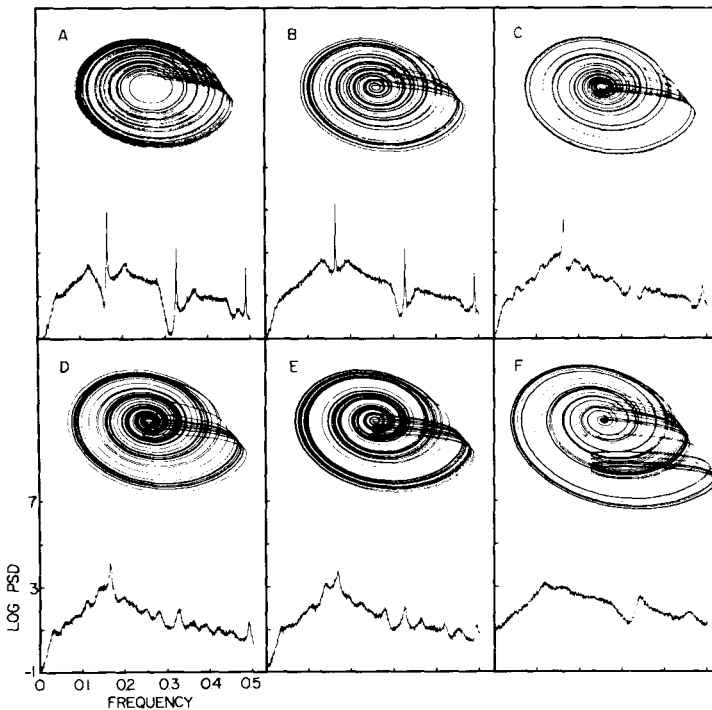


FIGURE 5. A bifurcation from instrumentally sharp phase coherence to incoherent behavior in the Rössler dynamical system (2). In each case, the power spectra were computed using $b = 0.4$ and $c = 8.5$; a is varied. (a) $a = 0.15$; the attractor is phase coherent with a spectrum similar to that of FIGURE 3b. (b) $a = 0.17$ (c) $a = 0.18$; the topology of the attractor is now like that of the funnel; the peak broadens as coherence is lost. (d) $a = 0.19$ (e) $a = 0.2$ (f) $a = 0.3$; trajectories now pass very close to the fixed point at the center of what used to be the hole; notice that the spectrum no longer drops off at zero frequency.

passage of time, the ensemble will grow in length at an exponential rate into a "filament" whose thickness (determined by the zero exponent) is roughly that of the initial distribution. Thus, mixing in directions transverse to the flow is guaranteed, and proceeds in a continuous manner. In contrast, mixing along the flow, and hence the coherence properties of an attractor, depends on the long-time behavior of these filaments.

To illustrate the differences between the mixing properties of phase coherent and phase incoherent attractors, we have made an animated movie. Unfortunately, the geographically distant reader will have to be content with FIGURES 6, 7, and 8. In each case, we begin with a finite ensemble of randomly selected points whose initial separation is on the order of 10^{-3} . This is small enough that the entire ensemble is initially visually indistinguishable from a single point. (The size of the attractor in each case is on the order of 10.) The trajectory of each point is integrated simultaneously, and the position of the points is displayed after varying intervals of time.

FIGURE 6a shows this on the Lorenz attractor after a sufficient time has passed for the ensemble to look like a filament. Notice how the filament is stretched by the saddle point in the bottom center of the figure (FIGURE 6b). After the passage of time very few points of the filament remain near the fixed point (FIGURE 6c). Although the filament is continuous in principle, it is effectively split into two fragments. Successive passes near the fixed point repeatedly split each fragment and the number of apparently distinct fragments grows exponentially. The cloud of points is very quickly distributed over the entire attractor (FIGURE 6f). No information about the initial time or position of the ensemble remains. This distribution now forms an experimental approximation to the relevant invariant measure of the attractor.

For the Lorenz attractor, the fixed point provides the mechanism that destroys phase coherence. This can be understood from two points of view:

1. Because points move very slowly when they pass close to the fixed point, small fluctuations can have a significant effect on the time it takes for them to pass the fixed point, and any coherence will be destroyed.
2. The splitting of filaments allows the ensemble to mix very quickly and cover the entire attractor. If, after the passage of a short time, a point can be found anywhere on the attractor, depending on the particular fluctuations it encounters or the exact location it had in the initial ensemble, then there can be no coherence to the motion.

With the approximation that the filamentary fragments seen in FIGURES 6c and 6d are distinct, explanation 2 easily leads to a random walk model for the loss of phase coherence. If the position within the initial localized ensemble is picked at random, then the fragment in which the point is located at a later time is also randomly selected. As is particularly apparent in FIGURE 6d, different fragments are associated with different "phases," in the sense that some fragments appear "ahead of" or "behind" others. Any fluctuation in the initial condition will create a distribution of phases that is approximately binomial and that, in the limit of many splittings, becomes Gaussian, in accordance with the central limit theorem. This implies that the phase coherence will be lost at an asymptotic rate of $t^{1/2}$, which is roughly what is observed in the numerical experiment of FIGURE 4.

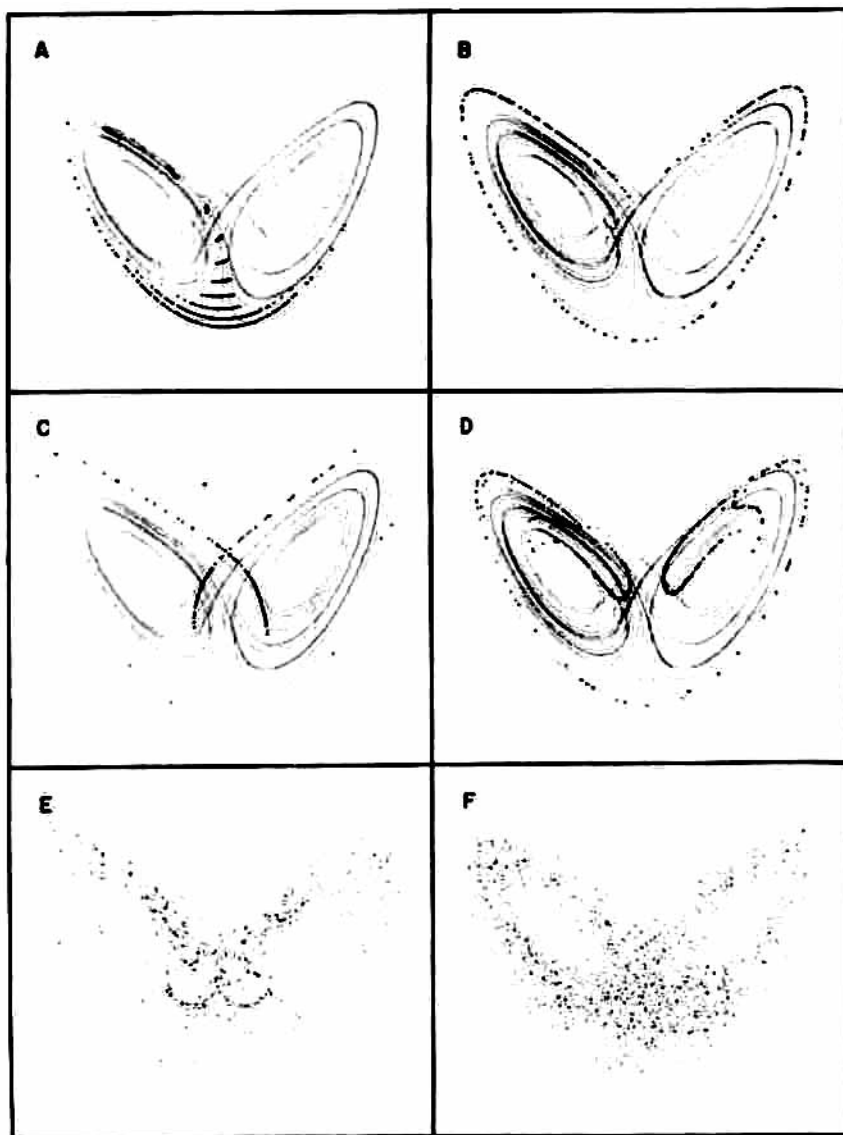
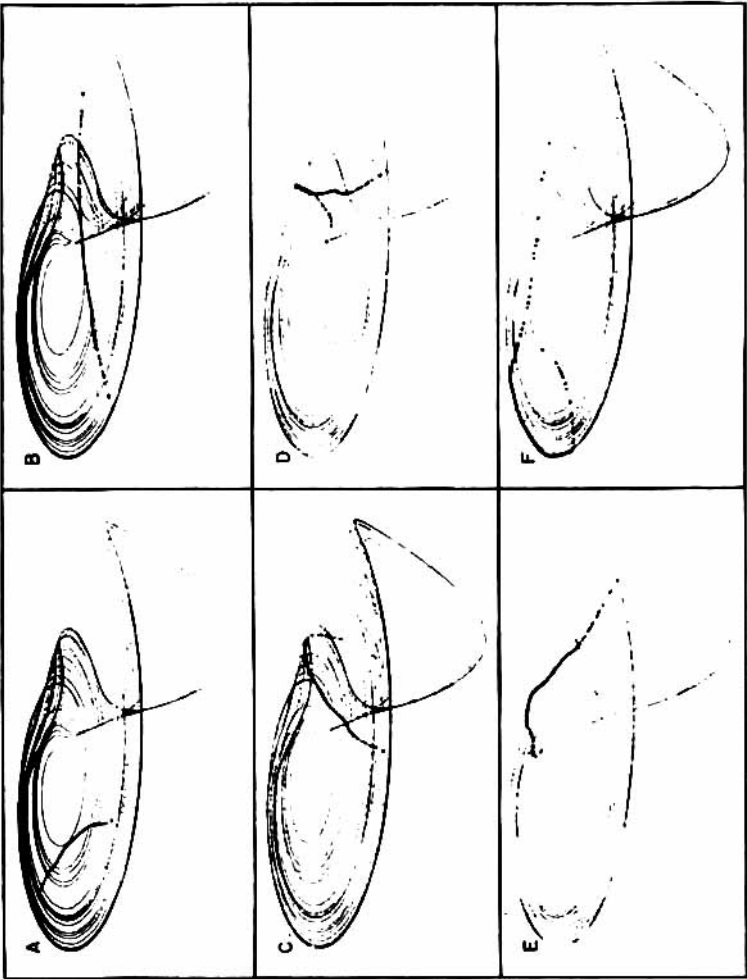


FIGURE 6. The mixing process of the Lorenz attractor. This illustrates the evolution of an ensemble of points that were initially close enough together to be visually indistinguishable from a single point. Each frame shows an xz projection of the ensemble after varying intervals of time. A sample trajectory is shown lightly in the background to outline the attractor. Time is given in units where the average time between maxima of z equals one, which may be thought of as "number of passes around the attractor." (a) Ten different strobos are shown, at times varying from $t = 6.9$ to $t = 7.8$. (b) One strobe, at $t = 8.2$. (c) $t = 8.5$. (d) $t = 12.1$. (e) $t = 18.2$. (f) $t = 27.7$. In a-c, each ensemble contains 256 points; in d and e, 1024 points; in f, 3072 points.



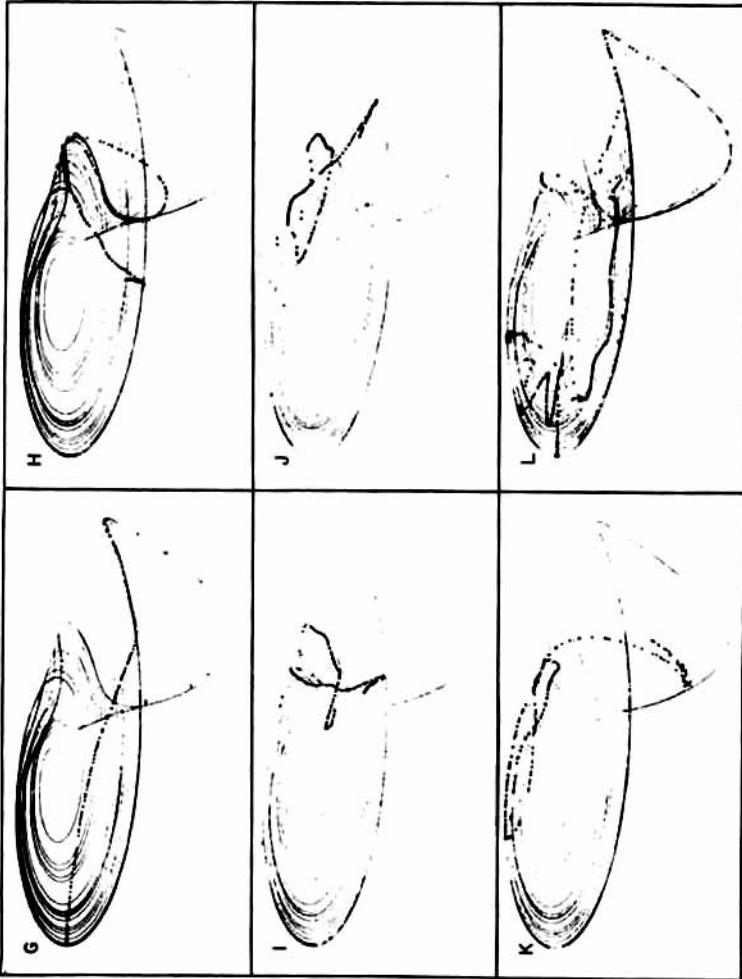


FIGURE 7. The mixing process of the funnel. The format is the same as for FIGURE 6, except that here we show a perspective view. (a) $t = 8.44$, (b) $t = 8.71$, (c) $t = 8.82$, (d) $t = 8.87$, (e) $t = 8.93$, (f) $t = 9.30$, (g) $t = 9.68$, (h) $t = 9.95$, (i) $t = 9.89$, (j) $t = 10.16$, (l) $t = 11.31$. All frames show 256 point ensembles, except l, which contains 1024 points.

Thus we see that a strange attractor containing a fixed point will mix rapidly and therefore be incoherent. However, this is not a necessary condition for incoherence, as can be seen by studying the funnel (FIGURE 7). For conceptual convenience, think of the attractor as being made of two parts, the "band" on the left of the figure, and the "funnel" on the right. As the ensemble passes the funnel, the part of the filament that was on the inside of the band emerges from the funnel before the part that was on the outside. When the entire filament emerges onto the band (FIGURE 7f), it is folded across the band. This process repeats itself until the filament takes on the complicated form seen in FIGURE 7i. In very little time, the ensemble approaches a smooth distribution that covers the entire attractor, just as it does in the case of the Lorenz attractor. Thus, this "asynchronous folding" is another mechanism that can bring about mixing.

In FIGURE 8, we illustrate the simple Rössler attractor, which, at least within the resolution of our experiments, is phase coherent. Notice that the filaments fold down close, but not exactly onto themselves (FIGURE 8c). Thus we see that asynchronous folding is not a sufficient condition for incoherence. After several more revolutions (FIGURE 8d), the filament crosses and recrosses itself. A comparison with the same experiment done on a limit cycle demonstrated that this phase spreading after 20 revolutions is not due to numerical errors. In spite of the initial spreading of the filament, after almost 5000 revolutions (FIGURE 8f) the ensemble remains confined and does not spread over the entire attractor. A comparison with a limit cycle after 5000 revolutions shows a similar amount of spreading due to numerical errors, demonstrating that the phase coherence of the simple Rössler attractor is comparable to that of a limit cycle. It is this confinement that preserves information about the initial phase and causes sharp peaks in the power spectrum. (The question now is, What causes the confinement?)

ISOCHRONS: A POSSIBLE EXPLANATION

One explanation for the phase coherence phenomenon might be that, for phase coherent dynamical systems, there always exists a coordinate transformation,

$$(x, y, z) \rightarrow (u, v, \theta),$$

after which the differential equations take the form

$$\left. \begin{aligned} \dot{u} &= f_u(u, v, \theta) \\ \dot{v} &= f_v(u, v, \theta) \\ \dot{\theta} &= \text{constant} \end{aligned} \right\} \text{periodic in } \theta. \quad (5)$$

This is the form of a periodically driven system for which many examples of chaotic behavior are known.^{16, 19} If such a transformation exists, then the attractor can be decomposed into subspaces where $\theta = \text{constant}$, or *isochrons* (FIGURE 9). Isochrons are mapped into one another by the flow and a given isochron is mapped into itself after some time T . For this reason, it is clear that an initially localized cloud of points cannot spread along the flow in such a system, since any spreading in the θ direction would imply that some isochrons were not being carried into themselves. Mixing can

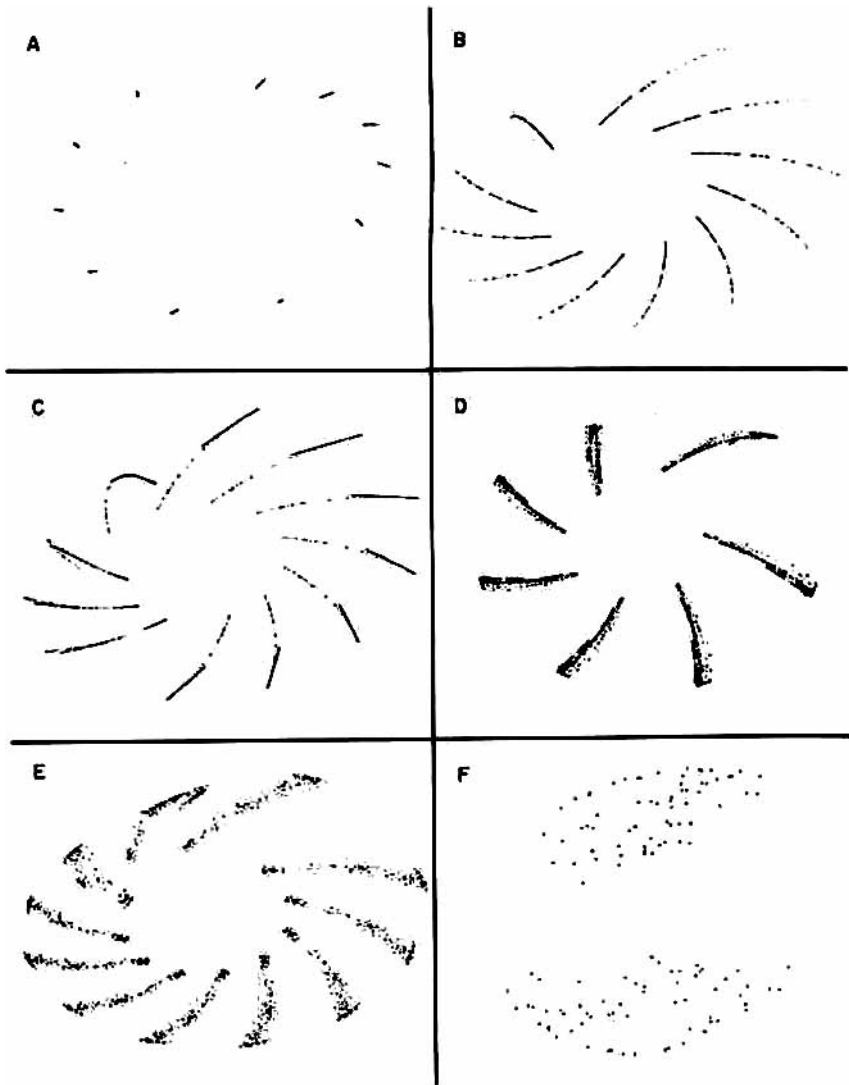


FIGURE 8. The mixing process of the simple Rössler attractor; xy projections of the evolution of an ensemble of initially neighboring points. (a) 11 stroboscopes, 64 points, beginning at $t = 6.8$. (b) 11 stroboscopes, 128 points, beginning at $t = 12.30$. (c) 11 stroboscopes, 256 points, beginning at $t = 13.67$. (d) 6 stroboscopes, 256 points, $t = 20$. (e) 11 stroboscopes, 256 points, $t = 159$. (f) 2 stroboscopes, 64 points, $t = 4723$.

only occur in the transverse direction to the flow. Driven oscillator systems are of this form by construction and they possess instrumentally sharp peaks in their power spectra at the driving frequency. Isochrons of stable limit cycles, which are, of course, phase coherent, are discussed in References 20 and 21. If a flow can be decomposed into isochrons, it is called a *constant time suspension*. (See Appendix III for a more detailed discussion.)

Bowen has proven that an Axiom A flow is a constant time suspension if and only if the flow is not mixing.²² Unfortunately, the simple Rössler attractor is not an Axiom A flow; we shall now discuss numerical evidence that indicates that the phase coherence of the simple Rössler attractor cannot be explained in terms of isochrons.

DOWNFALL OF ISOCHRONS

The fact that the folding of filaments is not synchronous, i.e., that the filaments of FIGURE 8 do not fold down onto themselves, even for the simple Rössler attractor,

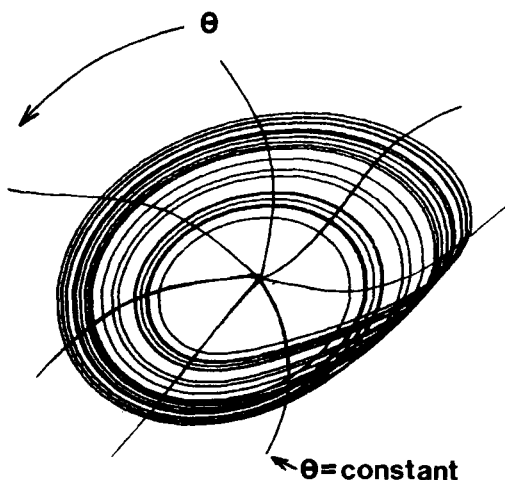


FIGURE 9. A schematic drawing showing hypothetical isochrons on an attractor such as the simple Rössler.

indicates that continuous isochrons do not exist. If continuous isochrons did exist, they would form a continuous family of nonintersecting curves on the attractor. Two neighboring points remain close to the same isochron. Thus, the spreading of an initially localized cloud of points would eventually trace out an isochron. The fact that the filaments seen in FIGURE 8d are not simple curves indicates that continuous isochrons do not exist.

However, since a cross section of a strange attractor reveals a fractal structure,^{23,24} one might suspect the existence of discontinuous isochrons, winding around on different leaves of the Cantor set structure. A demonstration that, even if they are discontinuous, isochrons cannot explain phase coherence is provided by the fact that the period of the unstable lowest-period limit cycle contained in the attractor is not the

same as the average period. (5.881 for the limit cycle versus 5.857 for the average period as measured from both maxima and zero crossings.) To be relevant to phase coherence, the period of the isochron must be the same as that of the fundamental peak in the power spectrum, which is the average period. But the isochron must also include a point on the unstable limit cycle, which leads to a contradiction. Thus, the long-term periodicity of the simple Rössler, and presumably of other examples, must be a statistical effect. A rough qualitative idea of how this comes about for the simple Rössler attractor can be garnered by examining FIGURE 8d. Although the filaments do not fold exactly onto themselves as they pass around the attractor, they do come close; the resulting tangled band is thin compared to the distance around the attractor. Furthermore, trajectories that take a longer time to get around the attractor tend to be followed by trajectories that take a shorter time. The standard deviation of the time for many cycles grows at a very slow rate. Presumably, then, the phase coherence of the Rössler is not perfect. Nevertheless, the phase spreading can be slow enough to be comparable to that of a limit cycle in the presence of small fluctuations.

Prediction and Time Evolution of the Entropy

If at some time an observation is made of a physical system, how precisely can the behavior of the system at some later time be predicted? An observation can never be made with infinite precision; at best a highly localized probability distribution can be prescribed. Thus, prediction must be discussed in terms of ensembles of initial conditions rather than in terms of the behavior of individual points. A natural way to do this is to partition the attractor by dividing it into a fine mesh of discrete cells. All the points within each cell may be lumped together to specify a "state" of the system, modeling the finite precision of a measuring instrument. This division, which is also sometimes called "coarse graining," enables one to make numerical computations and to assign a quantity of information or entropy to a continuous probability distribution.

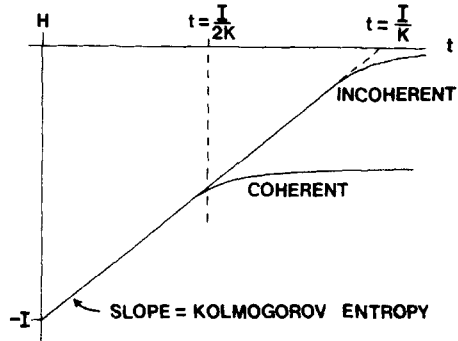
The entropy of a time-dependent distribution, $p(t)$, relative to the asymptotic distribution \bar{P} is

$$H_{\text{rel}}(t) = \sum_i p_i(t) \log \left(\frac{p_i(t)}{\bar{P}_i} \right), \quad (6)$$

where $\{p_i\}$ is the set of probabilities p_i induced by a partition of a continuous distribution p . For the examples we are considering, $p(t)$ describes the distribution of points in an ensemble. To an observer whose only knowledge of the state of the system is given by the asymptotic distribution of the attractor, the amount of new information gained in knowing the initial probability distribution is approximately $-H_{\text{rel}}(0)$. At time t , because of the action of the flow, this information will decay to $-H_{\text{rel}}(t)$; for a system that is mixing, $p(t) \rightarrow \bar{P}$ and $H_{\text{rel}} \rightarrow 0$ as $t \rightarrow \infty$. $H_{\text{rel}}(t)$ provides a quantitative measure of the information remaining after an observation.

On a strange attractor, if the system is isolated into a single state at $t = 0$, the number of states that are filled will, on the average, initially grow at a rate given by e^{kt} , where k is the Kolmogorov entropy of that attractor.^{16,24,25} Thus, the relative entropy will initially grow in a linear rate given by k , and, as long as there is no

FIGURE 10. Evolution of the relative entropy as a function of time for a phase coherent strange attractor and an incoherent attractor. For convenience, it is assumed that they have the same Kolmogorov entropy, k , and that the two coordinates needed to describe positions on the attractor are picked in such a way that the initial information, I , is divided evenly between them.



significant overlap between the resulting filaments, it will continue to grow at the same rate. However, once the filaments become sufficiently tangled, so that many of them are expanding into regions of the attractor that are already filled by others, this rate will decrease. (For examples, see FIGURES 6f and 7e. For a numerical demonstration with a one-dimensional map, see Shaw.¹⁸)

We can now infer the qualitative behavior of $H_{rel}(t)$ from the ensemble evolution experiments of FIGURES 6, 7, and 8. Let the information associated with the initial distribution of points be $I = -H_{rel}(0)$. Since the topological dimension of the attractors we are studying is two, the initial distribution can be described, in principle, by two coordinates. Assume for convenience that the initial information is divided evenly between them so that there is $I/2$ in each. Furthermore, imagine that coordinate patches are placed so that one of the coordinates is a phase coordinate that locally increases along the flow, and the other increases in directions transverse to the flow.

For attractors with broad spectra, such as the Lorenz attractor, the relative entropy $H_{rel}(t)$ increases at a linear rate equal to k until the attractor is almost covered and the relative entropy is close to zero. This occurs after a time I/k . (See Shaw.¹⁸) In contrast, for attractors with a high degree of phase coherence, although the initial rate of increase is equal to k , once the ensemble filaments cross the attractor several times, the rate of increase of the entropy becomes much smaller. At this point, which occurs roughly after a time $I/2k$, most of the transverse information is lost even though phase information persists (FIGURE 10).

For coherent attractors, then, phase information is lost at a rate significantly different from that of transverse information. The rate of loss of transverse information is an average local property. This rate is given by the Kolmogorov entropy, which is an average local measure, as may be seen through its relation to the positive Lyapunov exponents.^{11,12} For incoherent attractors, the rate of loss of phase information is closely coupled to the transverse information loss rate, for example by the action of a fixed point on the attractor. This coupling is absent, or at least weak, in coherent attractors. An example of the insensitivity of the Kolmogorov entropy to the propagation of phase information is provided by a comparison of the Lorenz and Rössler attractors: The Kolmogorov entropy of the Lorenz attractor has been directly measured to be 0.98, whereas the positive Lyapunov exponent of the simple Rössler attractor, which is believed to equal the Kolmogorov entropy, is 0.63.^{10,18} (Numbers are given in bits per crossing of a Poincaré section.) Thus, in the case of phase

coherence, the Kolmogorov entropy characterizes only the rate of transverse mixing, and not that for mixing along the flow.

POWER SPECTRAL MEASURES OF PHASE COHERENCE

Apparently, two strange attractors can have the same Kolmogorov entropy and yet have very different coherence properties. This indicates that the Kolmogorov entropy and the Lyapunov characteristic exponents are only partial indicators of the "chaotic properties" of a strange attractor. What is needed, then, is another measure that will distinguish between the coherence properties.

We have found two ad hoc measures that make this distinction. One of these, the "production of spectral entropy," has recently been reported on by Percival and Powell for Hamiltonian systems.²⁷ We call the other "production of new degrees of freedom." It is based on "degrees of freedom," a quantity that may be familiar from spectral analysis.²⁸ For N samples taken at intervals Δt of a record of length T ($N = T/\Delta t$), the number of degrees of freedom is

$$D(T) = \frac{\left(\sum_i^N S_i\right)^2}{\sum_i^N S_i^2}, \quad (7)$$

where S_i are the components of a power spectrum. Note that this quantity is unity for a perfectly sharp peak and N for white noise. The production of new degrees of freedom is defined to be

$$\frac{\Delta D}{\Delta T} = \frac{D(T_2) - D(T_1)}{T_2 - T_1}, \quad (8)$$

where $T_2 > T_1$. A practical computation of this measure gives a negative result for a periodic signal, a small but positive result for a coherently chaotic signal, and a significantly larger result for an incoherent signal. A few of our results are shown in TABLE 1. (We used $\Delta t = 0.1$, $T_2 = 409.6$, and $T_1 = 204.8$.)

CONCLUSIONS

A strange attractor can have an instrumentally sharp peak in a power spectrum. This means that, at least to a high degree of accuracy, the solution can be written as the sum of a periodic and a nonperiodic part, and that there is a nondecaying

TABLE 1

| Dynamical system | Production of new degrees of freedom = $\Delta D/\Delta T$ |
|----------------------------------|--|
| Rössler limit cycle | -6.4×10^{-5} |
| Simple Rössler strange attractor | 4.0×10^{-4} |
| Rössler funnel (FIGURE 5f) | 5.9×10^{-2} |

component of the autocorrelation function. We call this phenomenon phase coherence.

There is a continuum between coherent and incoherent behavior; bifurcations between the two are possible. However, in the bifurcation we observe, there appears to be a specific parameter value where incoherence sets in, which is associated with a change in the topology of the attractor.

The degree of phase coherence is related to the rate of mixing along the flow. A high degree of phase coherence indicates slow mixing along the flow, although the mixing transverse to the flow may be quite fast.

Kolmogorov entropy or Lyapunov exponents do not reflect the coherence properties of an attractor.

We have isolated two mechanisms that can bring about mixing along the flow:

1. a fixed point on the attractor
2. asynchronous folding.

1 is a sufficient condition for incoherence; 2 is not.

Phase coherence is often associated with a period-doubling bifurcation.

The loss of phase coherence for the Lorenz attractor proceeds at a rate of $t^{1/2}$, which can be understood in terms of a random walk model.

Phase coherent strange attractors are not necessarily constant time suspensions, or, in other words, phase coherence cannot in general be explained in terms of isochrons.

Care must be taken in using power spectra to determine the onset of turbulence (if it is due to dynamics), since, with limited experimental resolution, a phase coherent strange attractor may look like a limit cycle. For example, $z(t)$ of the simple Rössler attractor shows a sharp peak in the power spectrum six orders of magnitude above the broad background.

Phase coherence in a strange attractor may provide a good model for fluid flows that preserve large scale order on a background of small fluctuations.

QUESTIONS

What is the mechanism that causes phase coherence? Is there a topological or geometric condition that is sufficient to ensure instrumentally sharp phase coherence? For extremely coherent attractors, such as the simple Rössler or the Lorenz at $R = 200$, what is the intrinsic width of the spectral lines?

ACKNOWLEDGMENTS

We would like to thank Ralph Abraham, Bill Burke, David Fried, John Guckenheimer, and Joe Rudnick for valuable discussions. We would also like to thank Yoshitsugu Oono for stimulating correspondence, and Harry Swinney for his comments on the manuscript. Thanks are also due to Bud Bridges for the use of his microcomputer, the UCSC High Energy Physics group for the use of their NOVA minicomputer, and Jim Warner for valuable technical assistance.

REFERENCES

1. LORENZ, E. N. 1963. *J. Atmos. Sci.* **20**: 130.
2. RUELLE, D. & F. TAKENS. 1971. *Commun. Math. Phys.* **20**: 167.
3. RÖSSLER, O. E. 1976. *Phys. Lett. A* **57**: 397.
4. LORENZ, E. N. 1980. This volume.
5. ITO, K. Y. OONO, H. YAMAZAKI & K. HIRAKAWA. *Chaos in Seismology*. Preprint. Department of Earth Science, Kobe University. Nada, Kobe 657, Japan.
6. J. CRUTCHFIELD, D. FARMER, N. PACKARD, R. SHAW, G. JONES & R. J. DONNELLY. 1980. In press.
7. ARNOLD & AVEZ. 1968. *Ergodic Problems of Classical Mechanics*. W. A. Benjamin. New York.
8. BENNETIN, G., L. GALGANI & J.-M. STRELCYN. 1976. *Phys. Rev. A* **14**: 2338.
9. SHIMADA, I. & T. NAGASHIMA. 1979. *Prog. Theor. Phys.* **61**: 1605.
10. SHIMADA, I. 1979. *Prog. Theor. Phys.* **62**: 61.
11. PIESIN, YA. 1976. *Dokl. Akad. Nauk SSSR* **226**: 774. Translated in 1976. *Sov. Math. Dokl.* **17**: 196.
12. RUELLE, D. 1978. *Bol. Soc. Bras. Mat.* **9**: 83.
13. WALDEN, R. W. & R. J. DONNELLY. 1979. *Phys. Rev. Lett.* **43**: 301.
14. FENSTERMACHER, P. R., H. L. SWINNEY & J. P. GOLLUB. 1979. *J. Fluid Mech.* **94**: 103, especially Figure 5d.
15. RÖSSLER, O. E. 1977. *In Synergetics: A Workshop*. H. Haken, Ed.: 174. Springer Verlag. New York.
16. UEDA, Y. 1973. *Electron. Commun. Jpn.* **564**: 27.
17. HOLMES, P. J. 1977. *Appl. Math. Mod.* **1**: 362.
18. SHAW, R. S. 1980. *Proc. Transylvanian Phys. Soc.* Submitted.
19. HUBERMAN, B. & J. CRUTCHFIELD. 1979. *Phys. Rev. Lett.* **43**: 1743.
20. WINFREE, A. 1974. *J. Math. Biol.* **1**: 73.
21. GUCKENHEIMER, J. 1975. *J. Math. Biol.* **2**: 259.
22. BOWEN, R. 1972. *J. Math.* **94**: 1.
23. HENON, M. 1976. *Commun. Math. Phys.* **50**: 69.
24. MORI, H. 1980. *Prog. Theor. Phys.* **63**: (3).
25. GOLDSTEIN, S. *Entropy Increase in Dynamical Systems*. Preprint. Rutgers University.
26. OONO, Y. 1978. *Prog. Theor. Phys.* **60**: 1944.
27. PERCIVAL, I. & G. POWELL. 1979. *J. Phys. A* **12**: 2053.
28. BLACKMAN & TUKEY. 1959. *The Measurement of Power Spectra*. Dover.

APPENDIX I

This appendix contains a few details about numerical computations.

Unless otherwise stated, all simulations were done with Systron Donner model 3300 and model 10/20 analog computers. However, whenever there was any question of sensitivity to numerical errors, the computations were checked digitally to double precision.

The power spectra were obtained by taking a series of trials of 8192 samples of a given coordinate, each of which was then transformed using the fast Fourier transform. The sum of the squares of the real and imaginary parts of the Fourier components for a given frequency gives the power of that frequency component; to eliminate statistical fluctuations, many trials were averaged to yield a power spectrum for that frequency. The exact number of trials we used varies, but is typically 50, and never less than 10. To reduce side lobes in peaks, the signal was smoothed using a cosine bell over the first and last ten percent of the samples.

APPENDIX II

Using Fourier analysis, it is possible to infer an interesting property of the simple Rössler attractor at the parameter values of FIGURE 3. Notice the approximate symmetry of the broad component of the spectrum about the peaks in FIGURE 3b. The Fourier transform of the product of two functions is the convolution of the Fourier transform of each function. In particular, the convolution of a delta function located at w_0 with a broad function is a broad function symmetric about w_0 . This suggests that the nonperiodic part in equation 3 is the product of a chaotic part and a periodic part, $X_{NP} = X_P \cdot X_C$. It seems that, for this attractor, the following is true:

$$X(t) = X_P(t) [1 + X_C(t)] \quad (9)$$

This symmetric pattern is repeated around each harmonic of the sharp peak. However, the successive sidebands may overlap. The resulting pattern is dominated by the lower, stronger harmonic. This is apparently the reason for the one-sided repetition of the broad band between the harmonics.

APPENDIX III

This appendix outlines how isochrons are defined mathematically. A global cross section for a continuous flow $\Phi = \{\phi_t\}$ on a compact space M is a closed subset $S \subset M$ for which $\bigcup_{t \in (0, \alpha)} \phi_t S = M$ for some $\alpha > 0$ (the isochrons sweep across the entire state space), and $\bigcup_{t \in (0, \beta)} \phi_t S$ is an open subset of M disjoint from S for some $\beta > 0$ (the isochrons are, roughly speaking, transversal to the flow). There is then a homeomorphism $r: S \rightarrow S$ and a positive continuous function $u: S \rightarrow R$ given by

$$u(x) = \text{smallest time } t > 0 \text{ with } \phi_t x \in S$$

and

$$r(x) = \phi_{u(x)} x.$$

the map $r: S \rightarrow S$ is the "return map" for the section S and the flow ϕ is the suspension of r . u is the time of return function for the section S , so S is called an "isochron" if u is constant over S . In this case, Φ is a constant time suspension of r .